

# EEG-Based Cardiac Arrest Outcome Estimation with Highly Interpretable Features

Álvaro José Bocanegra<sup>1</sup>, Anaís Espinosa<sup>1</sup>, Ralph G. Andrzejak<sup>1</sup>, Oscar Camara<sup>1</sup>

<sup>1</sup> Universitat Pompeu Fabra, Barcelona, Spain

## Abstract

*The following is the solution proposed by the team UPFantastic for the Predicting Neurological Recovery from Coma After Cardiac Arrest: The George B. Moody PhysioNet Challenge 2023. The team was unable to be scored on the test set for the official phase of the challenge. Nevertheless, in our view, the methods proposed merit consideration, since the approach focused on interpretable features and analysis of the relevance and distribution of the data. We used synchrony and relative EEG band power measurements, along with patient data to feed a tree-based machine learning algorithm. We also used Multiple Kernel Learning in a subset to analyze the tendency of the patients during the monitoring in a dimensional reduced space.*

## 1. Introduction

The George B. Moody Physionet Challenge of this year focused on predicting the outcome of patients that suffered cardiac arrest. The outcomes were based on survival chances, and they were labeled as good or poor. Additionally, the challenge required to estimate the Cerebral Performance Category (CPC). The official score would be calculated using the True Positive Rate (TPR) at a False Positive Rate (FPR) not higher than 0.05 [1]. The provided dataset [2] had longitudinal data of electroencephalography (EEG), electrocardiography (ECG) and other relevant signals to analyze. The recordings were acquired during 72 hours after the patient suffered the cardiac arrest and the final prediction was reported using the full record.

We applied phase-locking measures for the extraction of the majority of features, which then served as inputs for the machine learning algorithm. The degree of synchrony has previously been shown to be useful in studying the absence of consciousness, as it is associated with a decrease in connectivity in patients with poor outcome [3]. Continuous EEG monitoring post-cardiac arrest uncovers distinct patterns, some of which mimic seizures. Such patterns, when observed in epilepsy studies, are associated

with synchronous neuronal activity in the brain [4].

Due to the complexity of the signal, it is possible to miss information when extracting features. Using dimensionality reduction (DR) techniques to work with these complex signals is recommended. Among the DR techniques, Multiple Kernel Learning (MKL) offers an interesting solution, since it allows to work with multiview and non-linear data, and it has been used in the biomedical signal analysis context before [5].

In the current work, we propose a highly interpretable solution for the classification of outcomes of cardiac arrest patients using EEG signals. We focused on feature extraction, using MKL to analyze patterns in the patients.

## 2. Materials and methods

### 2.1. Preprocessing

Based on previous work by Alnes *et al.* [6], we bandpass filtered the EEG signals within the  $\alpha$  range (8-15 Hz). Furthermore, given the intriguing patterns observed in the power spectrum within the  $\beta$  range (15-31 Hz) (see Fig. 1), we also opted to bandpass filter to this frequency range. The sampling frequency varied between 200 and 2500 Hz, depending on the recording. To reduce computational time, we downsampled the signals to achieve a new sampling frequency  $F_s$  of around 70 Hz. This strategy effectively prevented aliasing within the  $\beta$  range. EEG signals were referenced against the mean of all electrodes.

### 2.2. Channel selection

The EEG data was obtained using scalp electrodes following the International 10-20 system. Previous work [6] showed that the phase-locking between patients with good and poor outcomes differed more in the electrodes located in the frontal (Fp, F) and occipital (P, O) regions. Thus, we analyzed the signals registered from the Fp1, Fp2, F3, Fz, F4, P3, Pz, P4, O1, and O2 channels.

### 2.3. Relative energy

We used the power spectral density to quantify the distribution of energy across  $\alpha$  and  $\beta$  bands. The relative energy is a normalized measure to represent the contribution of a specific frequency band's energy with regard to the total energy across all bands. This is important since we compare the results across different patients. The relative energy  $E$  for a given frequency band is computed as:

$$E_\alpha = \frac{\int_{f_a}^{f_b} P(f) df}{\int_{f_0}^{f_1} P(f) df} \quad (1)$$

where  $f_0 = 0.5$  Hz and  $f_1 = Fs/2$  Hz, and  $f_a = 8$  and  $f_b = 15$  referring to the range of the  $\alpha$  band. The relative energy  $E_\beta$  in the  $\beta$  band is defined analogously for  $f_a = 8$  and  $f_b = 15$ .

### 2.4. Mean phase coherence

We quantified the degree of phase locking between signal pairs  $x(t_j)$  and  $y(t_j)$  consisting of  $N$  samples each taken at discrete times  $t_j$  for  $j = 1, \dots, N$  using the mean phase coherence  $R$  [7]. To do so, we first computed the instantaneous phase using the Hilbert transform  $\phi_x(t_j)$  and  $\phi_y(t_j)$  and determine their relative phase difference  $\varphi(t_j) = \phi_x(t_j) - \phi_y(t_j)$ . To measure the mean phase coherence, we evaluated the consistency of phase differences  $\varphi(t_j)$  using the order parameter:

$$R = \left| \frac{1}{N} \sum_{j=0}^{N-1} e^{i\varphi(t_j)} \right| \quad (2)$$

The measure attains values of  $R = 1$  if and only the phase difference  $\varphi(t)$  is equal during all time  $t$ , due to strong phase-locking. In contrast, when both dynamics are independent,  $R$  takes values close to zero.

### 2.5. Multivariate phase-locking

The mean phase coherence  $R$  only considers the phase-locking between signal pairs. We can modify Eq. 2 for obtaining the degree of phase-locking from  $L$  multivariate instantaneous phases  $k = 1, \dots, L$ :

$$Z = \frac{1}{N} \sum_{j=0}^{N-1} \left( \frac{1}{L} \left| \sum_{k=1}^L e^{i\varphi_k(t_j)} \right| \right) \quad (3)$$

If the dynamics underlying the measured time series  $x_1, \dots, x_L$  are independent,  $Z$  takes values close to zero. In contrast, we obtain  $Z = 1$  if and only if all  $L$  phases are equal at time  $t$ .

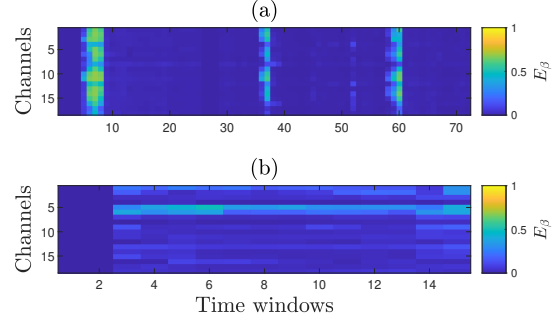


Figure 1: **Intermittent-like behavior was observed in the relative energy within the  $\beta$  range for a good outcome patient** (a) Relative energy  $E_\beta$  for exemplary good outcome patient for all electrodes and the 5 min with best signal to noise ratio of each hour after cardiac arrest. (b) Same as (a) for a poor outcome patient, where the energy pattern observed in (a) is not found.

### 2.6. Machine Learning

We split the dataset into training (70%) and validation (30%), the latter in turn was split to obtain a test subset (10% of the validation set). For both classification of the patient outcome and CPC score estimation, we used ensemble of bagged decision trees with 100 trees.

As input of the model, we used the patient features that were available: age, sex, return of spontaneous circulation (ROSC), out of hospital cardiac arrest (OHCA), shockable rhythm (SR), targeted temperature management (TTM) and features from the relative energy per channel, the bivariate and multivariate phase-locking.

### 2.7. Feature analysis

We applied the signal analysis techniques to the signals filtered in the  $\alpha$  and  $\beta$  ranges. We computed quantitative features, including the mean, maximum, and minimum of the measures. Additionally, we focused on temporal features to determine the specific time windows in which these quantitative features manifest. This information is relevant for predictions at 12, 24, 48 and 72 h. It is also relevant to identify the channels where these quantitative features occur most frequently. Therefore, we also derived certain spatial features. For instance, the signal pairs where the highest  $R$  value is more frequently obtained. Finally, some pattern-based features were derived from visual inspecting the measure results between patients with good outcomes and those with poor outcomes.

### 2.8. Multiple Kernel Learning

To analyze the signals we also used the MKL approach. This method calculates a different kernel for each feature

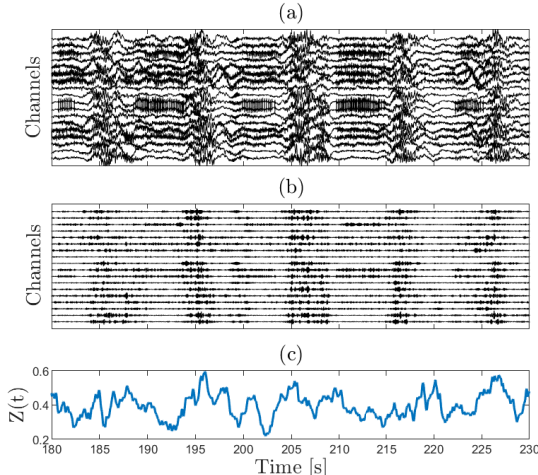


Figure 2: **Increased multivariate phase-locking observed in seizure-like patterns.** (a) Example 50-second windows from a patient with a good outcome with no filtering applied. (b) Same as (a) but applying a bandpass filter in the  $\alpha$  band. (c) Instantaneous multivariate phase-locking  $Z(t)$  computed for the data shown in (b). A 1-second moving average filter was applied to smooth the data for visual clarity.

and then computes a global affinity matrix that keeps similar inputs close in an output space [5]. We considered each channel as an independent feature and we included the original sampling frequency as the final input. Since this method does not scale well with large datasets, we lowered the computational cost by reducing the amount of data. First, we only applied the method on the test subset. Second, we applied the reduction techniques that we used for the classification: channel reduction and downsampling. Finally, inspired by the unofficial phase of the challenge, we decided to calculate the signal to noise (SNR) ratio of the signal in windows of 5 seconds. Then, we selected the 5 seconds window with the maximum quality of the record.

We performed the MKL training process, subsequently analyzing the output space. The original space had 10 features with 350 samples each and a single value for the original sampling frequency; after performing the MKL, the output space was reduced to 2 features, which allowed us to create a scatter plot of the dataset. We analyzed the different patient features and the outcomes in the output space. We also followed the trajectory of some cases to identify relevant biomarkers for the classifier.

### 3. Results

#### 3.1. Feature exploration

Fig. 1 shows the relative energy  $E_\beta$  derived from signals of a patient with a good outcome (Fig. 1a) and a poor

outcome (Fig. 1b). In the good outcome case, we observe a sporadic pattern of  $E_\beta$  peaks while in the poor outcome case, a different pattern is observed. We use this behavior to compute one of the features, which is the frequency of the outlier peak  $E_\beta$  occurrence. For Fig. 1a, we obtained 0.0667, and for Fig. 1b we get 0, which can be observed from the temporal energy evolution.

A further example is presented in Fig. 2, showing a seizure-like behavior recorded from a good outcome patient. This pattern is evident in both, in the broadband signal (Fig. 2a) and when filtered within the  $\alpha$  range (Fig. 2b). Computing the instantaneous multivariate phase-locking  $Z(t)$  allowed us to characterize approximately these patterns (Fig. 2c). Consequently, we used this high degree of phase-locking as one of the features extracted from the multivariate analysis.

#### 3.2. Classification

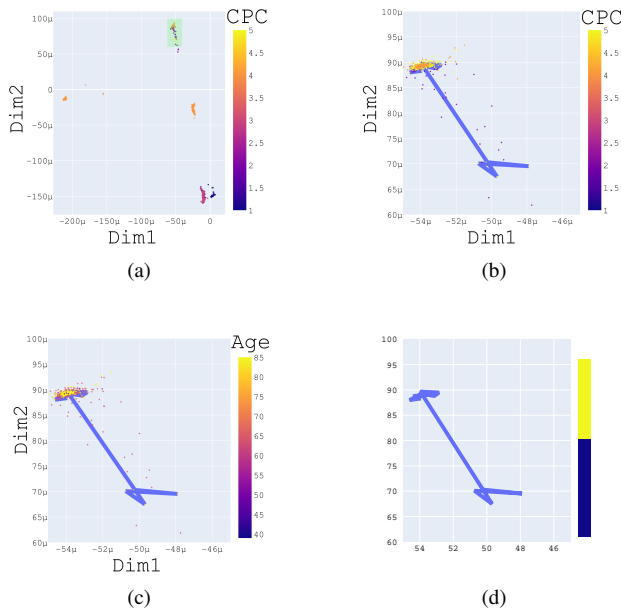
The scores reported in this section were acquired from the training set. The results during training were 100% for classification accuracy and 0.983 MSE for the regression model. The results for the validation subset were 75% of accuracy for the classification model and 2.555 MSE for the regression model. We used the specific scoring guidelines of the challenge in the test subset (see Table 1).

Table 1: Scores of the model using the challenge metrics in the test subset.

| Metric            | Score |
|-------------------|-------|
| Challenge Score   | 0.667 |
| Outcome AUROC     | 0.812 |
| Outcome AUPRC     | 0.894 |
| Outcome Accuracy  | 0.650 |
| Outcome F-measure | 0.627 |
| CPC MSE           | 1.251 |
| CPC MAE           | 0.918 |

#### 3.3. MKL

The scatter plot for the two first dimensions in the output space colored with the CPC values is shown in Fig. 3a. We colored the output space with the CPC values since it is noticeable the transition between zones with different outcomes. Since a patient has multiple records, we also wanted to see how the position of the patient changed in the output space through time, Fig. 3b shows the evolution of the patient 0341 through time. This patient had a poor outcome with a CPC score of 5. We show the same scatter plot comparing the trajectory with age, in Fig. 3c, and sex, in Fig. 3d. We did the same with other patients with other outcomes, resulting in unidirectional trajectories for poor



**Figure 3: Results on MKL implementation.** (a) Output space of the test dataset colored with the CPC values. (b) Left zoom of (a) (green box) in a specific zone of the output space. In the trajectory analysis, the first records are in the lower zone of the scatter plot, while the last records are in the upper zone. Finally, the same trajectory in the output space but colored with the ages (c) and sex (d) of the patients.

outcomes, as described in Fig. 3, and trajectories with no clear tendency for patients with an outcome with low CPC. Also, older patients and female patients showed a higher concentration on the final records of the poor outcomes trajectories. However, other features did not show clear trajectory patterns.

#### 4. Discussion and conclusions

We present an interpretable approach for classifying outcomes in cardiac arrest patients based on long-term EEG recordings. Although the score achieved is promising, it cannot be taken as valid as it was not evaluated on the hidden test set.

The features computed from the EEG analysis are consistent with previous studies [3, 6], since we obtained a higher degree of phase synchronization in patients with good outcome.

The MKL showed 4 clear clusters, two in the middle zone with high CPC scores, one with low CPC scores, and the last one with a mix between both possible outcomes. We used a patient of the latter to analyze the evolution of the signals for a poor outcome. Age and sex show changes

on the trajectory, passing from a mainly young and male zone with low density to a high-density zone with higher ages and more females. We did not see this pattern in the other patient features. On the one hand, the transition may illustrate how the survival chances of the patient change over time, which would be interesting to study for monitoring. On the other hand, the differences in the clinical features distribution could be related to the relevance of those features for the cluster formation in the output space, being age and sex the most relevant features.

Computing time is a limitation for this approach since both  $Z$  calculation and MKL training require high computational resources, which make them unfeasible for large scale databases. It is important to keep working on optimization methods for the implementation of both methods to solve this problem.

#### References

- [1] Reyna MA, Amorim E, Sameni R, Weigle J, Elola A, Bahrami Rad A, Seyedi S, Kwon H, Zheng WL, Ghassemi M, et al. Predicting neurological recovery from coma after cardiac arrest: The George B. Moody Physionet Challenge 2023. *Computing in Cardiology* 2023;50:1–4.
- [2] Amorim E, Zheng WL, Ghassemi MM, Aghaeeval M, Kandhare P, Karukonda V, Lee JW, Herman ST, Sivaraju A, Gaspard N, et al. The International Cardiac Arrest Research (I-CARE) Consortium Electroencephalography Database. *medRxiv* 2023;2023–08.
- [3] Carrasco-Gómez M, Keijzer HM, Ruijter BJ, Bruña R, Tjepkema-Cloostermans MC, Hofmeijer J, van Putten MJ. EEG functional connectivity contributes to outcome prediction of postanoxic coma. *Clinical neurophysiology* 2021; 132(6):1312–1320.
- [4] Fisher RS, Boas WVE, Blume W, Elger C, Genton P, Lee P, Engel Jr J. Epileptic seizures and epilepsy: definitions proposed by the International League Against Epilepsy (ILAE) and the International Bureau for Epilepsy (IBE). *Epilepsia* 2005;46(4):470–472.
- [5] Sanchez-Martinez S, Duchateau N, Erdei T, Fraser AG, Bijnsens BH, Piella G. Characterization of myocardial motion patterns by unsupervised multiple kernel learning. *Medical image analysis* 2017;35:70–82.
- [6] Alnes SL, De Lucia M, Rossetti AO, Tzovara A. Complementary roles of neural synchrony and complexity for indexing consciousness and chances of surviving in acute coma. *NeuroImage* 2021;245:118638.
- [7] Mormann F, Lehnertz K, David P, Elger CE. Mean phase coherence as a measure for phase synchronization and its application to the eeg of epilepsy patients. *Physica D Nonlinear Phenomena* 2000;144(3-4):358–369.

Address for correspondence:

Álvaro José Bocanegra Pérez  
 Universitat Pompeu Fabra, Barcelona, Spain  
 alvaro.bocanegra@upf.edu